JRMP Journal of Radiopharmaceuticals and Molecular Probes Vol. 5, No. 1, 2019
J Radiopharm Mol Probes 2019;5(1):54-60
ISSN 2384-1583(Print) / ISSN 2508-3848(Online)

ORIGINAL ARTICLE

https://doi.org/10.22643/JRMP.2019.5.1.54

Synthesis and evaluation of ^{64}Cu-labeled avidin for lymph node imaging

Choong Mo Kang,[1,†] Hyunjung Kim,[2] Yong Jin Lee,[3] and Yearn Seong Choe[1,2,*]

[1]Department of Nuclear Medicine, Samsung Medical Center, Sungkyunkwan University School of Medicine, Seoul, Korea
[2]Department of Health Sciences and Technology, SAIHST, Sungkyunkwan University, Seoul, Korea
[3]Division of Applied RI, Korea Institute of Radiological & Medical Sciences, Seoul, Korea

ABSTRACT

Sentinel lymph node (SLN) imaging plays an important role in surgery of patients with breast cancer and melanoma. In this study, avidin (Av), a tetrameric protein glycosylated with mannose and N-acetylglucosamine molecules, was labeled with ^{64}Cu and then evaluated for LN imaging. ^{64}Cu-Labeled NeutrAvidin™ (NAv), a non-glycosylated form of Av, was used for comparison. 1,4,7,10-Tetraazacyclododecane-N,N',N'',N'''-tetraacetic acid (DOTA)-conjugated Av and NAv were prepared from the corresponding proteins and DOTA-NHS ester, which were then labeled with copper-64 and purified using PD-10 columns. The numbers of DOTA molecules conjugated to Av and NAv were 4.9 and 3.3, respectively. [^{64}Cu]Cu-DOTA-conjugated Av and NAv were prepared in 93% and 73% radiochemical yields, respectively. In vitro serum stability study showed that copper-64 remained stable on all radiotracers for 24 h (>97%). MicroPET/CT images showed that high radioactivity was accumulated in LNs within 15 min after footpad-injection of radiotracers. Tissue distribution data of mice demonstrated significantly higher uptake in the popliteal (PO) LN than lumbar (LU) LN for ^{64}Cu-labeled Av (relative % ID/g excluding the injection sites: 66.2% and 26.0%, respectively) compared with those of ^{64}Cu-labeled NAv (43.0% and 49.2%, respectively). The results of this study suggest that mannose molecules on Av enabled the radiotracer to retain in the first LN after mouse footpad-injection.

Key Word: Sentinel lymph node, Avidin, NeutrAvidin, Copper-64, Mannose, PET/CT

Introduction

SLN imaging has an important role in determining the surgery regions of patients with breast cancer and melanoma, because of the involvement of SLN in metastasis. For SLN imaging, radiopharmaceuticals should have proper molecular sizes for efficient lymph drainage but not into blood drainage, ranging from 5 to 15 nm (1, 2). Of radiolabeled colloids, [^{99m}Tc]Tc-antimony sulfide colloid has fit into this size range, but [^{99m}Tc]Tc-sulfur colloid having rather large particle size (>100 nm) has shown slow radioactivity movement from the injection site (3). Considering the radioactivity retention in the SLNs, radiopharmaceuticals specifically targeting mannose receptors found on the surface of macrophages in LNs have been developed using mannose-conjugated dextran or human serum albumin (HSA) as a platform (4-9). Most notably, [^{99m}Tc]Tc-diethylenetriamine pentaacetic acid (DTPA)-mannosyl-dextran (Lymphoseek®) was shown to be

Received: June 7, 2019 / Revised: July 4, 2019 / Accepted: July 8, 2019

Correspnding Author : Yearn Seong Choe, Department of Nuclear Medicine, Samsung Medical Center, Sungkyunkwan University School of Medicine, 81 Irwon-ro, Gangnam-gu, Seoul 06351, Korea, Tel: 02-3410-2623, Fax: 02-3410-2667, E-mail: ysnm.choe@samsung.com

safe and effective for SLN imaging and was recently approved from the Food and Drug Administration (FDA) (4, 5). Since positron emission tomography (PET) is proven useful for early and accurate diagnosis of various diseases with high sensitivity and specificity, PET radiopharmaceuticals for SLN imaging are also on demand for development. ^{68}Ga- and ^{64}Cu-labeled mannosylated HSA showed potential for SLN imaging (8, 9). In addition, ^{64}Cu-labeled mannosylated HSA/indocyanine green (ICG) was also developed for preoperative PET/CT imaging and intraoperative near-infrared fluorescence detection of SLNs (9), because ICG, an FDA-approved dye, is easily adsorbed onto HSA (10).

Av is a tetrameric protein glycosylated with four to five mannose and three N-acetylglucosamine molecules at the Asn 17 residue of each monomer, which exists in more than three different oligosaccharide structural types (11). It is obtained from egg white and binds biotin with extremely high affinity (Kd ~ 10-15 nM) (12). In this study, Av was used as a platform for development of LN imaging agents, because it is glycosylated with mannose molecules that could be used for targeting mannose receptors in LNs. The non-glycosylated protein version of Av, NAv was used for comparison. NAv binds biotin as does Av, but it has low non-specific binding due to its low pI (6.3) and does not have mannose molecules (13). Therefore, we prepared ^{64}Cu-labeled Av and NAv to evaluate the effect of mannose molecules on Av in terms of LN imaging of mice using PET/CT.

Materials

Av and NAv were purchased from Life Technologies (Grand Island, NY, USA), and DOTA-NHS ester was from Macrocyclics (Dallas, TX, USA). [^{64}Cu]$CuCl_2$ was kindly provided by KIRAMS (Seoul, Korea). BCA protein assay kits were purchased from Pierce (Rockford, IL, USA), PD-10 columns were from Amersham Biosciences (Piscataway, NJ, USA), and Amicon filters were from Millipore (Billerica, MA, USA). All buffers used for synthesis and radiolabeling were pretreated with Chelex 100 resin (Merck, Darmstadt, Germany) to make metal-free conditions. Matrix-assisted laser desorption ionization time of flight (MALDI-TOF) mass spectrometry was performed on an AB SCIEX TOF/TOFTM 5800 System (Framingham, MA, USA).

Radioactivity was measured using a dose calibrator (Biodex Medical Systems, Shirley, NY, USA), and tissue radioactivity was measured using an automatic gamma counter (PerkinElmer, Waltham, MA, USA). MicroPET/CT images of mice were acquired using an Inveon microPET/CT scanner (Siemens Medical Solutions, Malvern, PA, USA). All animal experiments were performed in accordance with the National Institutes of Health Guide for the Care and Use of Laboratory Animals and were approved by the Institutional Animal Care and Use Committee of Samsung Medical Center.

Protocol

1. Preparation of DOTA-Av and DOTA-NAv

Av (1 mg, 16.6 nmol) was dissolved in 400 μL of 0.01 M sodium phosphate buffer (pH 7.4) and reacted with DOTA-NHS ester (157.6 or 333.3 μmol) in 100 μL of the same buffer. The reaction mixture was shaken at room temperature for 20 h and purified using a PD-10 column. The collected solution was concentrated using an Amicon 10K centrifugal filter and lyophilized. DOTA-NAv was synthesized by the same procedure described for the synthesis of DOTA-Av. DOTA-conjugated proteins were quantified using BCA protein assay kits, and then analyzed by MALDI-TOF mass spectrometry.

2. Preparation of [^{64}Cu]Cu-DOTA-Av and [^{64}Cu]Cu-DOTA-NAv

[^{64}Cu]$CuCl_2$ in 0.01 N HCl (50 μL, 157.44-210.16 MBq) was diluted with 200 μL of 0.1 M sodium acetate buffer (pH 6) and added to DOTA-Av (0.2 mg) in a 1.5-mL tube. The reaction solution was then stirred at 40 oC for 30 min and purified using a PD-10 column (saline). The aliquots (26.95-88.8 MBq/mL) of the collected fraction were concentrated using an Amicon 10K centrifugal filter, and the filtrate was diluted with saline and used for further experiments. [^{64}Cu]Cu-DOTA-NAv was synthesized by the same procedure described for the synthesis of [^{64}Cu]Cu-DOTA-Av.

3. In vitro serum stability

[^{64}Cu]Cu-DOTA-Av (38.33-39.15 MBq/500 μL) was added to 50% fetal bovine serum and incubated at 37 ˚C for 24 h. Aliquots were taken after 0, 1, 3, 16, and 24 h, and loaded onto PD-10 columns. The product fractions were eluted with 0.01 M PBS (pH 7.4) and counted using a dose calibrator. Percent (%) radioactivity was calculated relative to the radioactivity loaded onto the columns. Serum stability experiment of [^{64}Cu]Cu-DOTA-NAv was performed by the same procedure described for that of [^{64}Cu]Cu-DOTA-Av.

4. MicroPET/CT and PET imaging

[^{64}Cu]Cu-DOTA-Av and [^{64}Cu]Cu-DOTA-NAv (8.11 ± 0.62 MBq/50 μL) were injected into the left foot pads of ICR mice (male, 5-week-old, 29.65 ± 0.90 g, n = 3 per radiotracer). Dynamic PET images were acquired at 1-min intervals for 10 min, and additional computed tomography (CT) images were acquired for 20 min. Separately, PET images of ICR mice injected with ^{64}Cu-labled Av and NAv were acquired at 1-min intervals for 10 min. PET images were reconstructed using 3-D ordered subset expectation maximization and then processed using Siemens Inveon Research Workplace 4.2 (IRW 4.2).

5. Tissue distribution study

Immediately after microPET/CT imaging, mice were sacrificed and LNs (PO and LU) as well as other major organs were separated, weighed and counted. Data are expressed as relative % ID/g.

6. Statistical analysis

Data were analyzed using unpaired two-tailed Student's t-tests. Differences at the 95% confidence level ($P < 0.05$) were considered to be statistically significant.

Results

1. Preparation of DOTA-Av and DOTA-NAv

DOTA molecules were conjugated to Av and NAv, and the overall yields were 92.37% and 45.44%, respectively based on BCA protein assays. MALDI-TOF mass spectrometric analysis indicated that the average numbers of DOTA molecules conjugated to Av and NAv were 4.9 and 3.3, respectively. .

2. Preparation of [^{64}Cu]Cu-DOTA-Av and [^{64}Cu]Cu-DOTA-NAv

[^{64}Cu]Cu-DOTA-Av and [^{64}Cu]Cu-DOTA-NAv were prepared in high non-decay corrected radiochemical yields after purification using PD-10 columns (93% and 73%, respectively).

3. In vitro serum stability

In vitro serum stability analysis using PD-10 columns demonstrated that retention in percent radioactivity was observed for [^{64}Cu]Cu-DOTA-Av and [^{64}Cu]Cu-DOTA-NAv for 24 h. The remaining radiotracers were 97.01% and 98.76% at 0 h, 98.98% and 97.43% at 1 h, 99.16% and 98% at 3 h, 98.92% and 98.99% at 16 h and 98.69% and 97.07% at 24 h for 64Cu-labeled Av and NAv, respectively (Fig. 1). These results indicate

that copper-64 remained stable (>95% for 24 h) on the radiotracers during the period of this study.

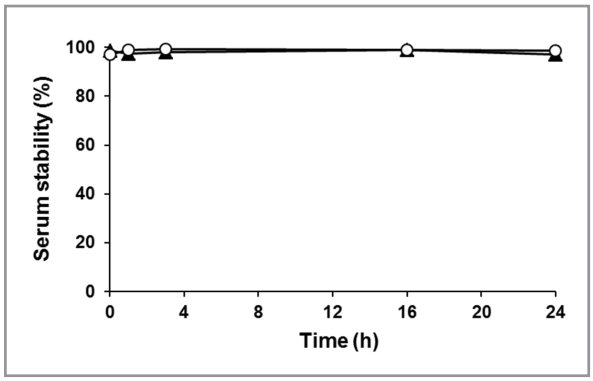

Figure 1. In vitro serum stability of [^{64}Cu]Cu-DOTA-Av (O) and [^{64}Cu]Cu-DOTA-NAv (▲)

4. MicroPET/CT and PET imaging

MicroPET/CT images of LNs in ICR mice were acquired for 30 min (10-min PET scan followed by 20-min CT scan) immediately after foot-pad injection of [^{64}Cu]Cu-DOTA-conjugated Av and NAv. Separate PET images were also acquired for 10 min. The PET/CT and PET maximum intensity projection (MIP) images are shown in Figs. 2a and 2b, respectively. High radioactivity uptakes were detected in the PO and the injection sites (left foot pad) in both PET/CT MIP images of mice (Fig. 2a). The radioactivity uptake in LU was much lower than that in PO in mice injected with [^{64}Cu]Cu-DOTA-Av, whereas other lymph nodes including LU were clearly shown in mice injected with [^{64}Cu]Cu-DOTA-NAv (Figs. 2a and 2b).

5. Tissue distribution

In tissue distribution study, high radioactivity was accumulated in the PO for [^{64}Cu]Cu-DOTA-Av. Data were expressed as relative % ID/g, and most of the radioactivity excluding that in the injection site was detected in the PO (66.2±3.2%) and LU (26.0±2.3%) after injection of [^{64}Cu]Cu-DOTA-Av (***P < 0.001) (Fig. 3a), and lower radioactivity was detected in the PO (43.0±2.4%) and LU (49.2±2.8%) after injection of [^{64}Cu]Cu-DOTA-NAv (**P < 0.01) (Fig. 3b). There was no radioactivity uptake in the contralateral PO and LU (Figs. 3a and 3b). The uptake ratio of PO to LU was 2.57±0.35 for [^{64}Cu]Cu-DOTA-Av, while that was 0.88±0.1 for [^{64}Cu]Cu-DOTA-NAv. The radioactivity uptake of both radiotracers was not significant in other tissues (liver, spleen, and kidneys).

Discussion

SLN imaging has been shown to be useful for the surgical decision-making of patients with breast cancer and melanoma. Radiopharmaceuticals

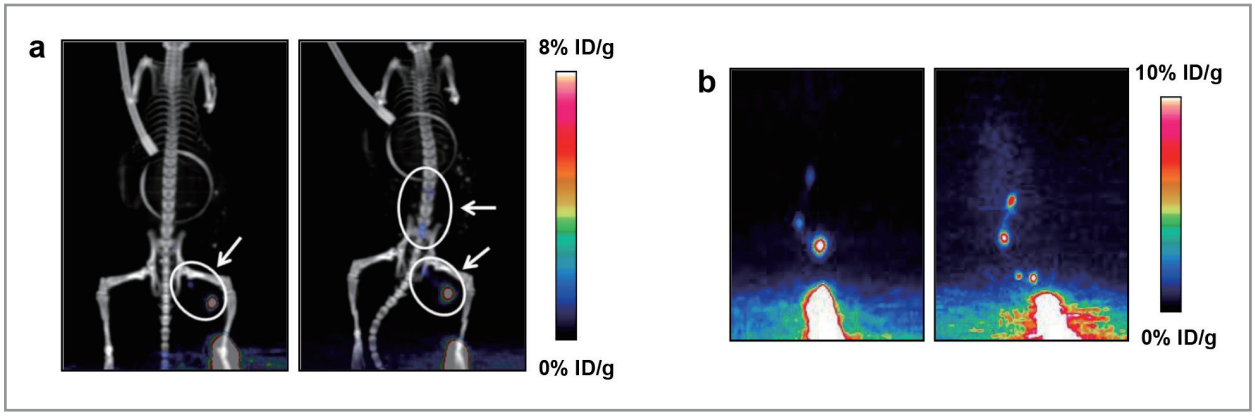

Figure 2. PET/CT MIP (a) and PET MIP images (b) of ICR mice obtained after injection of [^{64}Cu]Cu-DOTA-Av (let) and [^{64}Cu]Cu-DOTA-NAv (right) (10-min PET scan followed by 20-min CT scan (a); 10-min PET scan (b))

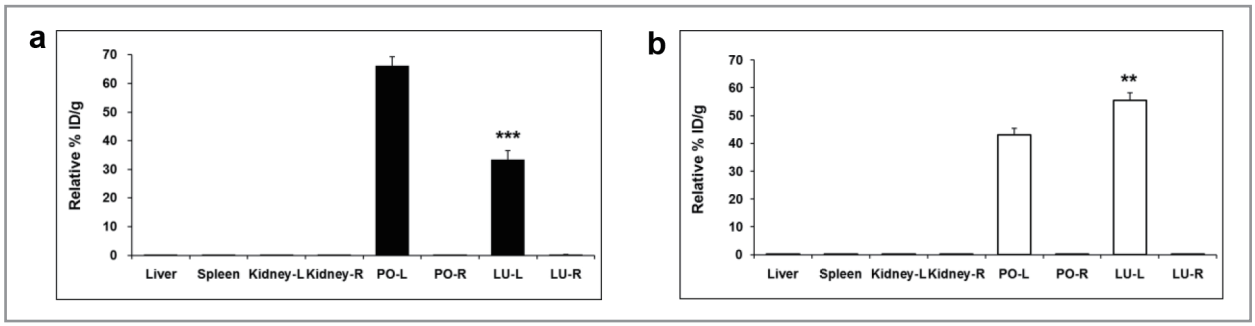

Figure 3. Tissue distribution of [^{64}Cu]Cu-DOTA-Av (a) and [^{64}Cu]Cu-DOTA-NAv (b). PO: popliteal; LU: lumbar (**P < 0.01, ***P < 0.001)

for SLN imaging should have proper molecular size and targeting efficiency. Proper sizes of radiopharmaceuticals are reported to range from 5 to 15 nm (1, 2). Av falls within the proper size with 7.2 nm (maximum cross-section) and 5.4 nm (hydrodynamic diameter by dynamic light scattering measurement) (14). The specific targeting of LNs can be efficiently obtained using radiopharmaceuticals that can bind to mannose receptors on the surface of macrophages in LNs. Therefore, mannose-conjugated radiotracers have been developed for SLN imaging. [^{99m}Tc] Tc-DTPA-mannosyl-dextran, the FDA-approved radiopharmaceutical for SLN detection, has 55 mannose molecules per dextran based on measurement using the sulfuric acid method (4, 15). In the cases of ^{68}Ga- and ^{64}Cu-labeled mannosylated HSA, MALDI-TOF mass spectrometry data showed that average 10.6 and 7.17 mannose molecules were conjugated to HSA, respectively (8, 9). Av is a tetrameric protein glycosylated with four to five mannose molecules per monomer, although mannose molecules most likely exist as oligosaccharide and hybrid forms (11). ^{64}Cu-labeled Av was therefore considered as a radiotracer for specific targeting of LNs, due to the presence of mannose molecules glycosylated to Av. SPECT radiopharmaceuticals specifically targeting mannose receptors include Lymphoseek® and ^{99m}Tc-labeled nanocoll, which demonstrated appropriate properties for SLN imaging (4, 16). Recently, PET radiotracers for SLN imaging have been also reported; ^{68}Ga- and ^{64}Cu-labeled mannosylated HSA (8, 9).

In the present study, Av and NAv were labeled with copper-64 via DOTA molecules, because copper-64 has been widely used for radiolabeling of proteins and peptides. In order to prepare DOTA-conjugated Av and NAv, 10 or 20 equivalents of DOTA-NHS ester were added to Av and NAv, respectively. The numbers of DOTA molecules conjugated to Lys residues of NAv were 3.3, which were lower than those of Av (4.9) based on analysis using MALDI-TOF mass spectrometry. This difference may be attributed to different spatial locations of Lys residues in Av and NAv. High radiochemical yields were obtained for [^{64}Cu]Cu-DOTA-conjugated Av and NAv (73-93%). The in vitro stability analysis demonstrated that both radiotracers were stable in serum over 24 h (Fig. 1). Dynamic PET imaging for the first 10 min was performed in ICR mice after subcutaneous injection of radiotracer into the foot pads (Fig. 2). [^{64}Cu]Cu-DOTA-conjugated Av and NAv were rapidly accumulated in the PO after the foot-pad injection. In the tissue distribution study, higher radioactivity uptake by the PO than by the LU was observed for [^{64}Cu]Cu-DOTA-Av (ratio, 2.57±0.35) than for [^{64}Cu]Cu-DOTA-NAv (ratio, 0.88±0.1), which may be attributed to the presence of mannose molecules in the former. As expected, [64Cu]Cu-DOTA-Av showed higher retention of radioactivity in the first lymph node after foot-pad injection than [^{64}Cu] Cu-DOTA-NAv.

Conclusion

We synthesized ^{64}Cu-labeled Av and NAv for PET/CT imaging of LNs. In vivo results suggest that the number of mannose molecules in Av may not be sufficient to retain [^{64}Cu]Cu-DOTA-Av longer in the first LN after footpad-injection, although higher rate of leakage from the LN was observed in [^{64}Cu]Cu-DOTA-NAv that does not contain mannose molecules. Further studies to improve the retention of ^{64}Cu-labeled Av in the first LN (PO) are underway to investigate the effect of mannose molecules on uptake of LN using [^{64}Cu]Cu-DOTA-mannose-conjugated Av.

Acknowledgements

This research was supported by the National Research Foundation of Korea grant funded by the Korean government (2017M2A2A7A01070487) and a grant of the Korea Institute of Radiological and Medical Sciences (KIRAMS), funded by Ministry of Science and ICT (MSIT), Republic of Korea (No. 50536-2019).

References

1. Henze E, Schelbert HR, Collins JD, Najafi A, Barrio JR, Bennett LR. Lymphoscintigraphy with Tc-99m-labeled dextran. *J Nucl Med* 1982;23:923-9.
2. Strand SE, Person BRR. Quantitative lymphoscintigraphy I: Basic concepts for optimal uptake of radiocolloids in the parasternal lymph nodes of rabbits. *J Nucl Med* 1979;20:1038-46.
3. Stern HS, McAfee JG, Subramanian G. Preparation, distribution and utilization of technetium-99m-sulfur colloid. *J Nucl Med* 1966;7:665-75.
4. Vera DR, Wallace AM, Hoh CK, Mattrey RF. A synthetic macromolecule for sentinel node detection: [^{99m}Tc]DTPA-mannosyldextran. *J Nucl Med* 2001;42:951-9.
5. Wallace AM, Hoh CK, Vera DR, Darrah DD, Schulteis G. Lymphoseek: a molecular radiopharmaceutical for sentinel node detection. *Ann Surg Oncol* 2003;10:531-8.
6. Jeong JM, Hong MK, Kim YJ, Lee J, Kang JH, Lee DS, Chung JK, Lee MC. Development of ^{99m}Tc-neomannosyl human serum albumin (^{99m}Tc-MSA) as a novel receptor binding agent for sentinel lymph node imaging. *Nucl Med Commun* 2004;25:1211-7.
7. Takagi K, Uehara T, Kaneko E, Nakayama M, Koizumi M, Endo K, Arano Y. ^{99m}Tc-labeled mannosyl-neoglycoalbumin for sentinel lymph node identification. *Nucl Med Biol* 2004;31:893-900.
8. Choi JY, Jeong JM, Yoo BC, Kim K, Kim Y, Yang BY, Lee YS, Lee DS, Chung JK, Lee MC. Development of ^{68}Ga-labeled mannosylated human serum albumin (MSA) as a lymph node imaging agent for positron emission tomography. *Nucl Med Biol* 2011;38:371-9.
9. Kang CM, An GI, Choe YS. Hybrid lymph node imaging using ^{64}Cu-labeled mannose-conjugated human serum albumin with and without indocyanine green. *Nucl Med Commun* 2015;36:1026-34.
10. Moody ED, Viskari PJ, Colyer CL. Non-covalent labeling of human serum albumin with indocyanine green: a study by capillary electrophoresis with diode laser-induced fluorescence detection. *J Chromatogr B* 1999;729:55-64.
11. Bruch RC, White HB III. Compositional and structural heterogeneity of avidin glycopeptides. *Biochemistry* 1982;21:5334-41.
12. Green NM. Avidin. In: Anfinsen CB, Edsall JT, Richard FM, editors. Advances in Protein Chemistry. New York: Academic Press; 1975. p. 85-133.
13. Marttila AT, Laitinen OH, Airenne KJ, Kulik T, Bayer EA, Wilchek M, Kulomaa MS. Recombinant NeutraLite Avidin: a non-glycosylated, acidic mutant of chicken avidin that exhibits high affinity

for biotin and low non-specific binding properties. FEBS Lett 2000;467:31-6.

14. Liljeström V, Mikkilä J, Kostiainen MA. Self-assembly and modular functionalization of three-dimensional crystals from oppositely charged proteins. *Nat Commun* 2014;5:4445.
15. Dubios M, Gilles KA, Hamilton JK, Rebers PA, Smith F. Colorimetric method for determination of sugars and related substances. *Anal Chem* 1956;28:350-6.
16. Gommans GMM, Gommans E, van der Zant FM, Teule GJJ, van der Schors TG, de Waard JW. ^{99m}Tc Nanocoll: A radiopharmaceutical for sentinel node localisation in breast cancer - *In vitro* and in vivo results. *Appl Radiat Isot* 2009;67:1550-8.